Throughput Performance of Iterative Frequency-domain SIC with 2D MMSE-FDE for SC-MIMO Multiplexing

Akinori Nakajima† and Fumiyuki Adachi‡
Dept. of Electrical and Communications Engineering, Graduated school of Engineering,
Tohoku University, Sendai, Japan
†nakajima@mobile.ecei.tohoku.ac.jp, ‡adachi@ecei.tohoku.ac.jp

Abstract— **Broadband wireless packet access will be the core technology of the next generation mobile communication systems. For very high-speed and high-quality packet transmissions in a limited bandwidth, the joint use of multiple-input multiple-output (MIMO) multiplexing and hybrid ARQ (HARQ) is an effective method. However, if single-carrier (SC) transmission is used, the transmission performance significantly degrades due to a large inter-symbol interference (ISI) resulting from a severe frequency-selective fading. In this paper, we propose an iterative frequency-domain successive interference cancellation (SIC) with two dimensional (2D) MMSE-FDE. At each iteration stage, the successive signal detection/cancellation is performed according to the descending order of the signal reliability. However, since the interference from the other transmit antennas can be only partially cancelled by performing SIC, the residual interference is present at the output of SIC. In this paper, we propose to update the 2D MMSE-FDE weights at each signal detection in order to suppress simultaneously the ISI and the interference from other antennas while obtaining antenna and frequency diversity gain. However, since a single use of SIC with 2D MMSE-FDE is insufficient, it is repeated a sufficient number of times. The bit error rate (BER) and HARQ throughput performance in a frequency-selective Rayleigh fading channel are evaluated by computer simulation.**

Keywords- SC-MIMO multiplexing, Iterative frequency-domain SIC, 2D MMSE-FDE, RCPT-HARQ

I. INTRODUCTION

Recently, there have been tremendous demands for high-speed data transmissions higher than few tens of Mbps in mobile communications [1]. However, for such high-speed data transmissions, the channel consists of many resolvable paths with different time delays, resulting in a severely frequency-selective fading channel. The transmission performance of SC transmission significantly degrades due to a severe inter-symbol interference (ISI) [2]. Recently, it has been shown that the use of frequency-domain equalization (FDE) can significantly improve the SC transmission performance [3,4]. For wireless communication, however, the available bandwidth is limited, so some highly spectrum-efficient transmission technique is required for the next generation mobile communication systems. One of the promising techniques is the multiple-input multiple-output (MIMO) multiplexing [5], that uses multiple transmit and receive antennas. Packet access will be the core technology of the next generation mobile communication systems. For very high-speed and high-quality packet transmissions in a limited bandwidth, the joint use of MIMO multiplexing and hybrid automatic repeat request (HARQ) is very effective.

In MIMO multiplexing, the transmit data sequence is transformed into parallel sequences and each sequence is transmitted from a different transmit antenna at the same time with the same carrier frequency. Therefore, the total transmission data rate increases in proportion to the number of transmit antennas without requiring additional bandwidth. At a receiver, it is necessary to separate the signals transmitted from different antennas. A lot of research attention has been paid to develop the signal separation schemes, which provide a performance close to that of maximum likelihood detection (MLD) but with reduced complexity, like vertical-Bell laboratories layered space-time architecture (V-BLAST) [6] (which is a version of successive interference cancellation (SIC)), MLD using QR decomposition [7] and so on.

Recently, we had proposed an iterative frequency-domain parallel interference cancellation (PIC) with two dimensional minimum mean square error (2D MMSE)-FDE for single carrier (SC)-MIMO multiplexing in a frequency-selective fading channel [8,9]. In 2D MMSE-FDE, the FDE weight is considered for each pair of transmit antenna and receive antenna. However, in PIC, all interference replicas are generated at the same time and therefore, an interference replica having low reliability limits the performance improvement. Another cancellation scheme is successive interference cancellation (SIC). In SIC, signal detection/cancellation is performed according to the descending order of the signal reliability. Therefore, the interference replica is more reliable than in PIC and hence, SIC provides better performance than PIC. In this paper, we propose an iterative frequency-domain SIC with 2D MMSE-FDE for SC-MIMO multiplexing in a frequency-selective fading channel. For the separation of the transmitted signals, the successive signal detection/cancellation is performed at each iteration stage according to the descending order of the signal reliability. However, since SIC can cancel only partially the interference from the other transmit antennas, the residual interference is present at the output of SIC. In this paper, the 2D MMSE-FDE weights are updated, by using the signals which have already been detected, at every signal detection in order to suppress simultaneously the ISI and the residual interference from other antennas while obtaining antenna and frequency diversity gain. However, since the initial iteration stage can not sufficiently suppress the interference, frequency-domain SIC with 2D MMSE-FDE is repeated a sufficient number of times. We evaluate, by computer simulation, the bit error rate (BER) performance and the throughput performance of rate compatible punctured turbo coded (RCPT) HARQ [10] of SC-MIMO multiplexing using iterative frequency-domain SIC with 2D MMSE-FDE in a frequency-selective Rayleigh fading channel. We then compare the BER and throughput performances of the proposed SIC with those of PIC [8,9].

The remainder of this paper is organized as follows. Section II describes the iterative frequency-domain SIC with 2D MMSE-FDE. In section III and IV, the system model and RCPT-HARQ are explained, respectively. Section V presents the computer simulation results of the BER and throughput performances. Section VI concludes this paper.

II. ITERATIVE FREQUENCY DOMAIN SIC WITH 2D MMSE-FDE FOR SIGNAL SEPARATION

At the receiver, a superposition of the all transmitted signals is received. Therefore, it is necessary to separate the transmitted signals. In this paper, an iterative signal separation method using FDE based on MMSE criterion is considered. Joint equalization and signal separation is performed simultaneously by applying 2D MMSE-FDE. By this operation, the transmitted signals can be separated while obtaining the frequency diversity gain.

The iterative frequency-domain SIC with 2D MMSE-FDE is illustrated in Fig.1. It is composed of 1) ordering, 2) soft decision & frequency-domain SIC and 3) 2D MMSE-FDE. At the initial iteration stage (i=0), the transmitted signal, which has the highest channel gain of all undetected signals, is detected by performing 2D MMSE-FDE. Then, the replica of the signal, which has been just detected, is generated and is subtracted from the received signals. A new 2D MMSE weight vectors for the undetected signals are computed again and one of these signals is detected. Until all the transmitted signals are detected, SIC with 2D MMSE-FDE is performed. However, since a single use of SIC with 2D MMSE-FDE can not suppress sufficiently the ISI and the interference from other antennas, this is repeated a sufficient number of times.

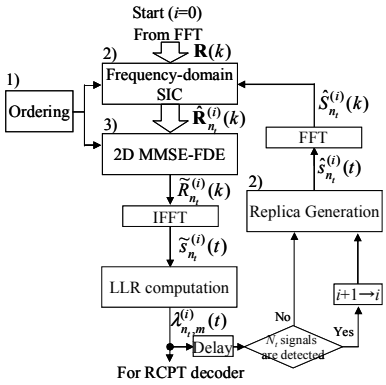

Figure 1 Iterative frequency-domain SIC with 2D MMSE-FDE at the ith stage.

III. SYSTEM MODEL

A. Transmitted and received signal representation

Fig.2 shows the transmitter/receiver structure of SC-(N_t,N_r)MIMO multiplexing with iterative frequency-domain SIC using 2D MMSE-FDE. N_t transmit and N_r receive antennas are used. At the transmitter, turbo coding is performed on the CRC coded binary information sequence and the transmitted sequences obtained by puncturing the turbo coded sequence are stored in the buffer. In this paper, RCPT type II HARQ [11] is considered.

After the bit-interleaving and data-modulation, for MIMO multiplexing, the data-modulated symbol sequence is serial-to-parallel (S/P) converted to N_t parallel sequences, each to be transmitted from a different transmit antenna. In this paper, QPSK data-modulation is considered. Each QPSK modulated symbol sequence is divided into a sequence of blocks of N_c symbols each. The data symbol, transmitted from the n_tth antenna at time t, is denoted by $s_{n_t}(t)$, where t=0~N_c-1. The last N_g symbols in each block are copied and inserted as a cyclic prefix into the guard interval (GI), placed at the beginning of each block, to form a frame with (N_g+N_c) symbols.

N_t symbol blocks are transmitted simultaneously in parallel from N_t transmit antennas using the same carrier frequency. At the receiver, a superposition of N_t transmitted signals is received by N_r antennas via a frequency-selective fading channel. The channel is assumed to be a symbol-spaced L-path frequency-selective fading channel, each discrete propagation path being subjected to independent fading. After the removal of the GI from the received signal, N_c-point fast Fourier transform (FFT) is applied to decompose the GI-removed received signal $r_{n_r}(t)$, t=0~N_c-1, into N_c frequency components. The kth frequency component $R_{n_r}(k)$ of the received SC signal on the n_rth antenna is expressed as

$$R_{n_r}(k) = \sqrt{2S}\sum_{n_t=0}^{N_t-1} H_{n_r,n_t}(k) S_{n_t}(k) + \Pi_{n_r}(k), \quad (1)$$

where S is the received signal power per antenna, $H_{n_r,n_t}(k)$ is the complex channel gain between the n_tth transmit antenna and the n_rth receive antenna, $S_{n_t}(k)$ is the transmitted signal component, and $\Pi_{n_r}(k)$ is the noise component. They are given by

$$\begin{cases} H_{n_r,n_t}(k) = \sum_{l=0}^{L-1} h_{n_r,n_t,l} \exp(-j2\pi\tau_l k/N_c) \\ S_{n_t}(k) = \sum_{t=0}^{N_c-1} s_{n_t}(t) \exp(-j2\pi t k/N_c) \\ \Pi_{n_r}(k) = \sum_{t=0}^{N_c-1} n_{n_r}(t) \exp(-j2\pi t k/N_c) \end{cases}, \quad (2)$$

where $h_{n_r,n_t,l}$ denotes the lth path gain between the n_rth receive antenna and n_tth transmit antenna, $n_{n_r}(t)$ is a zero-mean complex Gaussian process having a variance $2\sigma^2 = 2N_0/T_s$ with N_0 being the one-sided power spectrum density of additive white Gaussian noise (AWGN) and T_s being the symbol length.

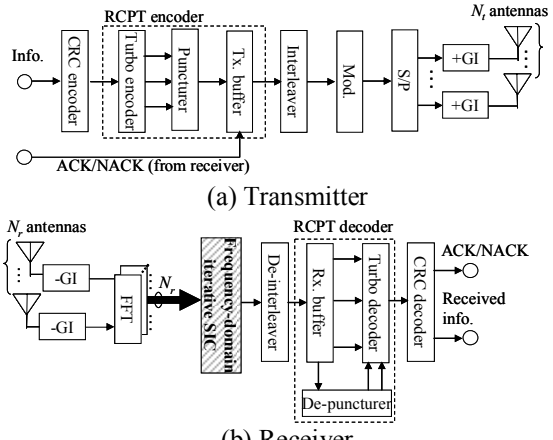

(a) Transmitter

(b) Receiver

Figure 2 Transmitter/receiver structure.

B. Iterative frequency-domain SIC with 2D MMSE-FDE

1) Ordering

In this paper, the signal detection is performed according to the descending order of the equivalent channel gain. In what follows, without loss of generality, the transmit antenna having the highest equivalent channel gain is assumed to be the 0th transmit antenna, followed by the 1st, 2nd, …, (N_t-1)th antennas. The equivalent channel gain of the n_tth transmit antenna in the ith iteration is given by

$$\hat{H}_{n_t}^{(i)} = (1/N_c)\sum_{k=0}^{N_c-1} \overline{H}_{n_t,n_t}^{(i)}(k) \text{ , (3)}$$

where

$$\overline{H}_{n_t,n_t'}^{(i)}(k) = \mathbf{w}_{n_t}^{(i)}(k)\mathbf{H}_{n_t'}(k) \text{ , (4)}$$

where $\mathbf{H}_{n_t'}(k) = [H_{0,n_t'}(k),\cdots,H_{N_r-1,n_t'}(k)]^T$ is N_r-by-1 channel gain vector between the n_t'th transmit antenna and all receive antennas at the kth frequency and is the n_t'th column vector of N_r-by-N_t complex channel gain matrix $\mathbf{H}(k)$. $\mathbf{w}_{n_t}^{(i)}(k) = [w_{0,n_t}^{(i)}(k),\cdots,w_{N_r-1,n_t}^{(i)}(k)]^T$ is 1-by-N_r 2D MMSE weight vector for the n_tth transmit antenna in the ith iteration. Until all the transmitted signals are detected, ordering is carried out at every signal detection.

2) Soft replica generation & frequency-domain SIC

The time-domain received symbol block $\{\tilde{s}_{n_t}^{(i)}(t)$; t=0~N_c-1$\}$ is obtained by performing N_c-point IFFT on $\{\tilde{R}_{n_t}^{(i)}(k)$; k=0~N_c-1$\}$ after carrying out 2D MMSE-FDE in the ith iteration. Then, the log likelihood ratio (LLR), $\lambda_{n_t,b}^{(i)}(t)$, of the the mth bit $b_{n_t,m}(t)$ in the tth symbol transmitted from the n_tth transmit antenna is computed by using $\tilde{s}_{n_t}^{(i)}(t)$, as [12]

$$\lambda_{n_t,m}^{(i)}(t) \approx \frac{1}{2\overline{\sigma}_{n_t}^{(i)^2}} \left(\begin{array}{l} \left|\tilde{s}_{n_t}^{(i)}(t) - \sqrt{2S}\hat{H}_{n_t}^{(i)}\bar{s}_{b_{n_t,m}(t)=0}^{\min}\right|^2 \\ -\left|\tilde{s}_{n_t}^{(i)}(t) - \sqrt{2S}\hat{H}_{n_t}^{(i)}\bar{s}_{b_{n_t,m}(t)=1}^{\min}\right|^2 \end{array} \right) \text{, (5)}$$

where $\bar{s}_{b_{n_t,m}(t)=0}^{\min}$ ($\bar{s}_{b_{n_t,m}(t)=1}^{\min}$) is the most probable symbol whose mth bit is 0 (or 1), for which the Euclidean distance from $\tilde{s}_{n_t}^{(i)}(t)$ is minimum. $\overline{\sigma}_{n_t}^{(i)^2}$ is the variance of the interference and noise component and given by

$$\overline{\sigma}_{n_t}^{(i)^2} = S\left[\begin{array}{l} \left\{(1/N_c)\sum_{n_t'=0}^{N_t-1} g_{n_t,n_t'}^{(i)} \sum_{k=0}^{N_c-1}\left|\overline{H}_{n_t,n_t'}(k)\right|^2\right\} - \left|\hat{H}_{n_t}\right|^2 \\ +(S/\sigma^2)^{-1}(1/N_c)\sum_{k=0}^{N_c-1}|\overline{\Pi}_{n_t}^{(i)}(k)|^2 \end{array} \right] \text{, (6)}$$

where

$$\overline{\Pi}_{n_t}^{(i)}(k) = \sum_{n_r=0}^{N_r-1} w_{n_r,n_t}^{(i)}(k)\Pi_{n_r}(k) \text{ (7)}$$

is the noise after 2D MMSE-FDE. $g_{n_t,n_t'}^{(i)}$ reflects the contribution of interference from the n_t'th transmit antenna to the n_tth transmit antenna.

The soft replicas, $\{\hat{s}_{n_t}^{(i)}(t)\}$, n_t=0~N_t-1, to be used for the next detection are generated by using $\{\lambda_{n_t,m}^{(i)}(t)\}$ [8,9]. N_c-point FFT is performed on $\{\hat{s}_{n_t}^{(i)}(t)$; n_t=0~N_t-1$\}$ to obtain the frequency-domain signal replica $\{\hat{S}_{n_t}^{(i)}(k)$; k=0~N_c-1$\}$. Then, SIC is performed to extract the frequency component $\hat{R}_{n_t,n_r}^{(i)}(k)$ of the n_tth block as

$$\hat{R}_{n_t,n_r}^{(i)}(k) = R_{n_r}(k) - \sqrt{2S}\sum_{n_t'=0\neq n_t}^{N_t-1}\left\{ H_{n_r,n_t'}(k)\times\left\{ \begin{array}{l}(1-\varepsilon_{n_t'}^{(i)})\hat{S}_{n_t'}^{(i-1)}(k) \\ +\varepsilon_{n_t'}^{(i)}\hat{S}_{n_t'}^{(i)}(k)\end{array}\right\}\right\} \text{ . (8)}$$

Since the blocks with $n_t' < n_t$ have already been detected, their replicas are generated using the decision feedback of the present ith iteration (i.e., $\hat{S}_{n_t'}^{(i)}(k)$ for $n_t' < n_t$) and $\varepsilon_{n_t'}^{(i)}$=1 for $n_t' < n_t$. However, the blocks with $n_t' > n_t$ are undetected and hence, their replicas are generated using the decision feedback of at the (i-1)th iteration (i.e., $\hat{S}_{n_t'}^{(i-1)}(k)$ for $n_t' > n_t$) and $\varepsilon_{n_t'}^{(i)}$=0 for $n_t' > n_t$.

3) 2D MMSE-FDE

The kth frequency component of the n_tth block after 2D MMSE-FDE is denoted by $\tilde{R}_{n_t}^{(i)}(k)$ and is expressed as

$$\tilde{R}_{n_t}^{(i)}(k) = \mathbf{w}_{n_t}^{(i)}(k)\hat{\mathbf{R}}_{n_t}^{(i)}(k) \text{ , (9)}$$

where $\hat{\mathbf{R}}_{n_t}^{(i)}(k) = [\hat{R}_{n_t,0}^{(i)}(k),\cdots,\hat{R}_{n_t,N_r-1}^{(i)}(k)]^T$ is the N_r-by-1 received signal vector after SIC. $\mathbf{w}_{n_t}^{(i)}(k)$ is given as

$$\mathbf{w}_{n_t}^{(i)}(k) = \mathbf{H}_{n_t}^H(k)[\mathbf{H}(k)\mathbf{G}_{n_t}^{(i)}\mathbf{H}^H(k) + (E_s/N_0)^{-1}\mathbf{I}]^{-1} \text{, (10)}$$

where $(.)^H$ is the Hermitian transpose operation, $\mathbf{I}$ is the N_r-by-N_r identity matrix. E_s/N_0 represents the average received symbol energy-to-AWGN power spectrum density ratio per receive antenna. $\mathbf{G}_{n_t}^{(i)} = diag[g_{n_t,0}^{(i)},\cdots,g_{n_t,N_t-1}^{(i)}]$ is an N_t-by-N_t diagonal matrix, where $g_{n_t,n_t'}^{(i)}$ is given by

$$g_{n_t,n_t'}^{(i)} = \begin{cases} 1 & \text{if } n_t' = n_t \\ 1 - \dfrac{1}{N_c}\displaystyle\sum_{t=0}^{N_c-1}\left\{ \begin{array}{l}(1-\varepsilon_{n_t'}^{(i)})\,|\,\hat{s}_{n_t'}^{(i-1)}(t)\,|^2 \\ +\varepsilon_{n_t'}^{(i)}\,|\,\hat{s}_{n_t'}^{(i)}(t)\,|^2\end{array}\right\} & \text{otherwise} \end{cases} \text{ . (11)}$$

Setting $\varepsilon_{n_t}^{(i)}$ to 1, the (n_t+1)th block is detected. After all the transmitted blocks are detected, the next iteration is carried out.

The above processes 1)~3) are repeated a sufficient number of times. Then, deinterleaving and RCPT decoding are performed. In the RCPT decoder, depuncturing, turbo decoding, and error detection are performed. The result of error detection is transmitted to the transmitter as ACK/NACK.

IV. RCPT TYPE II HARQ

In this paper, RCPT type II HARQ [11] is applied. Turbo encoder of coding rate R=1/3 is considered. The turbo encoder outputs the systematic bit (information bit) sequence and two parity bit sequences, each has a length of K bits. In this paper, type II S-P2 is considered. In what follows, S-P2 is explained. The schematic diagrams are shown in Fig.3. The 1st transmit packet consists of the systematic bit sequence only and the 2nd and 3rd are taken from two punctured parity bit sequences. The following puncturing matrices are used for the 1st, 2nd and 3rd transmissions [11]:

$$\begin{bmatrix} 1 & 1 \\ 0 & 0 \\ 0 & 0 \end{bmatrix}, \begin{bmatrix} 0 & 0 \\ 1 & 0 \\ 0 & 1 \end{bmatrix}, \begin{bmatrix} 0 & 0 \\ 0 & 1 \\ 1 & 0 \end{bmatrix}.$$

Fig.4 shows HARQ protocols. At the transmitter, the first packet, consisting of systematic bit sequence only, is transmitted. At the receiver, error detection is performed. If any error is detected in the received packet, an NACK is transmitted to the transmitter. Then, the second packet is transmitted. At the receiver, depuncturing is performed, followed by turbo decoding. In this case, turbo coding corresponds to R=1/2. After turbo decoding, the error detection is performed. If any error is detected, the receiver transmits the NACK again. At the transmitter, another punctured parity bit sequence is transmitted. At the receiver side, the second and third received packets are transformed into two parity bit sequences by depuncturing and then, R=1/3 turbo decoding is carried out again.

V. COMPUTER SIMULATION

The simulation parameters are given in Table 1. We assume an information bit sequence of K=2048 bits. Coding rate R=1/3 turbo encoder, consisting of two (13,15) recursive systematic convolutional (RSC) encoders, is employed. We assume N_r-by-N_t independent and identically distributed frequency-selective block Rayleigh fading channels and each channel has a symbol-spaced exponentially decaying L=16-path power delay profile with decay factor α. Ideal channel estimation is assumed. Each transmit symbol block is composed of N_c=256 symbols and the GI length is N_g=32 symbols.

The uncoded BER performance of SC-(4,4)MIMO multiplexing is plotted in Fig.5 as a function of the average received energy per bit-to-noise power spectrum density ratio E_b/N_0 per receive antenna. It can be seen that the BER performance with both SIC and PIC improves, but the additional improvement becomes smaller as the number of iterations increases. In SIC, the use of 2 iterations is sufficient. On the other hand, PIC requires 3 and 2 iterations when α=0 and 6dB, respectively. When α=0dB, the required E_b/N_0 for the average BER=10^{-4} is only slightly less with SIC (i=2) than with PIC (i=3). However, when α=6dB, SIC can reduce the required E_b/N_0 by about 0.8dB compared to PIC.

The throughput performance of RCPT type II HARQ S-P2 for SC-(4,4)MIMO multiplexing is plotted in Fig.6 as a function of the average received energy per symbol-to-noise power spectrum density ratio E_s/N_0 per receive antenna. SIC and PIC provide similar throughput performance when α=0dB (strong selectivity); however, the former provides much higher throughput performance when α=6dB (weak selectivity). The required E_s/N_0 with SIC for a throughput of 6.5 bps/Hz is about 2.7 dB smaller than with PIC. In the case of α=6dB (weak selectivity), the accuracy of interference replicas degrades since the channel gains at many frequencies fade simultaneously. As a consequence, the throughput performance degrades compared to the case of α=0dB (strong selectivity). However, SIC provides better throughput performance, even using a lower number of iterations, than PIC.

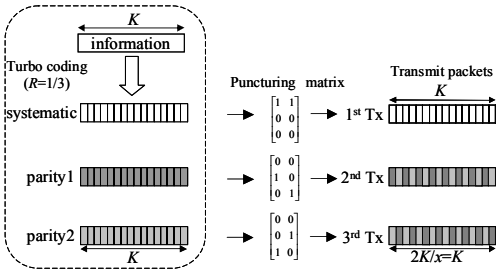

Figure 3 Transmit packet generation for RCPT type II HARQ S-P2.

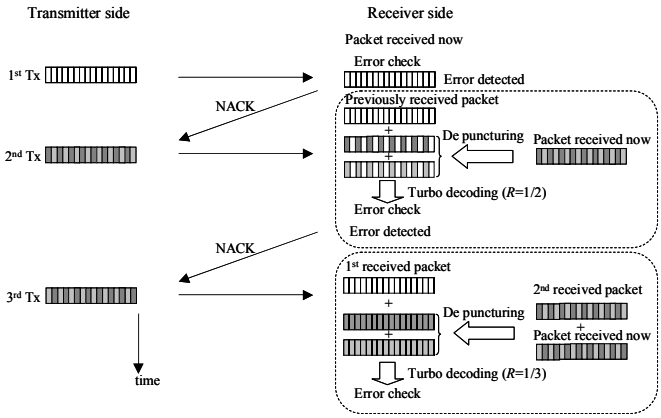

Figure 4 HARQ protocol.

Table 1. Simulation conditions.

Data Modulation		QPSK
Number of Tx, Rx Antennas		N_t=N_r=4
Number of FFT points		N_c=256
GI		N_g=32
Channel	Frequency-selective block Rayleigh fading	
	L=16-path exponential power delay profile	
	Decay factor α=0, 6dB	
Channel estimation		Ideal

VI. CONCLUSIONS

In this paper, we proposed iterative frequency-domain SIC with 2D MMSE-FDE for SC-MIMO multiplexing. The successive signal detection/cancellation is performed according to the descending order of the equivalent channel gain after 2D MMSE-FDE. 2D MMSE weights are updated at every signal detection to suppress simultaneously the ISI and the residual interference from other antennas while obtaining

antenna and frequency diversity gain. However, only the initial iteration stage can not suppress the interference from other antennas. Therefore, to improve the signal separation, SIC with 2D MMSE-FDE is repeated a sufficient number of times. We evaluated, by computer simulation, the BER and throughput performance with SIC in a frequency-selective Rayleigh fading channel and compared them with those of PIC. It was shown that although SIC provides only slightly better throughput performance than PIC when α=0 dB (strong frequency-selective channel), the superiority of SIC over PIC is significant when α=6 dB (weak frequency-selective channel) and the required E_s/N_0 is smaller by about 2.7 dB.

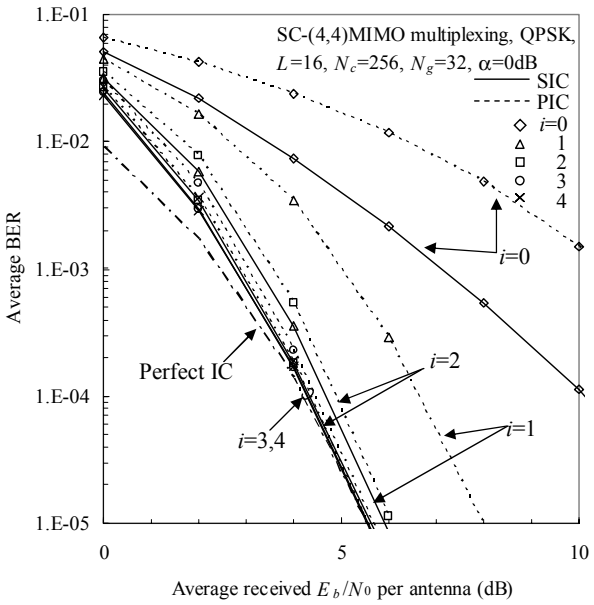

(a) α=0dB

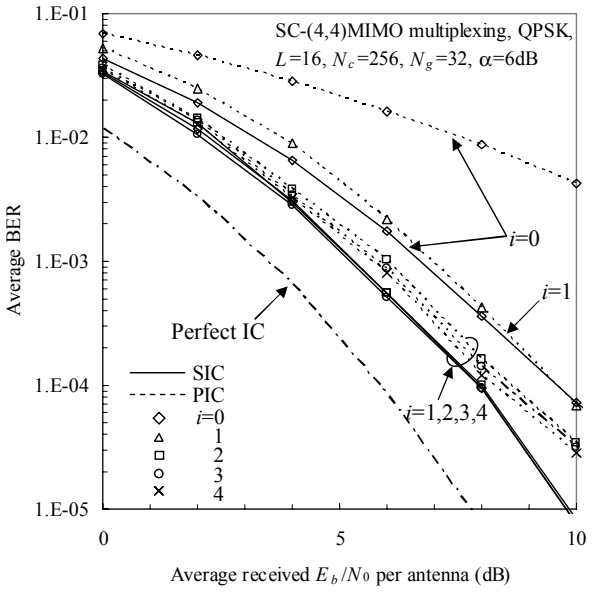

(b) α=6dB

Figure 5 BER performance.

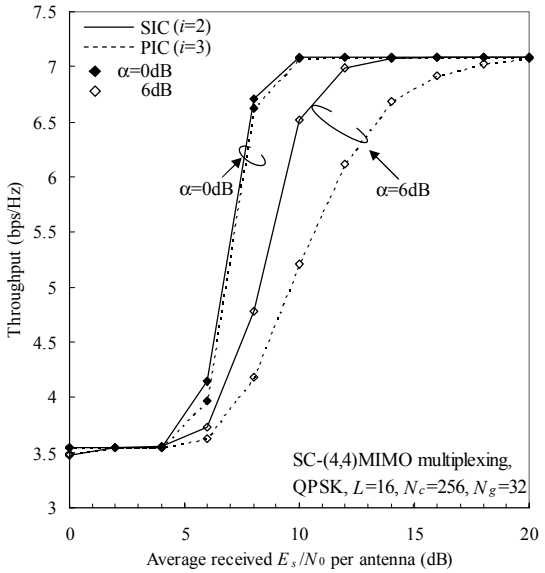

Figure 6 Throughput performance of HARQ typeII S-P2.

REFERENCES

[1] F. Adachi, "Wireless past and future-evolving mobile communications systems," IEICE Trans. Fundamentals, vol.E83-A, No.1, pp.55-60, Jan. 2001.

[2] John G. Proakis, *Digital Communications*, 4th edition, McGraw-Hill, 2001.

[3] D. Falconer, et al., "Frequency domain equalization for single-carrier broadband wireless systems," IEEE Commun. Mag., vol.40, pp.58-66, April 2002.

[4] F. Adachi, D. Garg, S. Takaoka, and K. Takeda, "Broadband CDMA techniques," Special Issue on Modulation, Coding and Signal Processing, IEEE Wireless Commun. Mag., Vol. 12, No. 2, pp. 8-18, April 2005.

[5] G. J. Foschini, et al., "On of wireless communications in a fading environment when using multiple antennas," Wireless Personal Communi., Vol.6, No. 3, pp. 311-335, Mar. 1998.

[6] P. W. Wolniansky, et al., "V-BLAST: an architecture for realizing very high data rates over the rich-scattering wireless channel," Proc. ISSSE, pp.295-300, Italy Sept. 1998.

[7] H. Kawai, et al., "Likelihood function for QRM-MLD suitable for soft-decision turbo decoding and its performance for OFCDM MIMO multiplexing in multipath fading channel," IEICE Trans. Commun., vol E88-B, No.1, pp.47-57, Jan. 2005.

[8] J. Hagenauer, et al., "Rate-compatible punctured convolutional codes (RCPC codes) and their application," IEEE Trans. Commun., vol. 36, no. 4, pp.389-400, April 1988.

[9] A. Nakajima, et al., "Iterative PIC using 2D MMSE-FDE for Turbo-coded HARQ with SC-MIMO multiplexing," Proc. IEEE VTC2006-Spring, Melbourne, Australia, April 2006.

[10] A. Nakajima, et al., "Throughput of turbo coded hybrid ARQ using single-carrier MIMO multiplexing," Proc. IEEE VTC2005-Spring, Stockholm, Sweden, April 2005.

[11] D. Garg, et al., "Rate compatible punctured turbo-coded hybrid ARQ for OFDM in a frequency selective fading channel," Proc. IEEE VTC2003-Spring, pp.2725-2729, Jeju, Korea, April 2003.

[12] A. Stefanov, et al., "Turbo coded modulation for wireless communications with antenna diversity," J. Commun. Netw., vol. 2, no. 4, pp. 356-360, Dec. 2000.